Preparation and Luminescence Properties of Polymers Containing Dialkoxyacenes

Mu-Lin Tsai and Ching-Yang Liu

Department of Applied Chemistry, Chinese Culture University, Taipei, Taiwan

Ya-Yun Wang, Jao-yu Chen, and Teh-Chang Chou*

Department of Chemistry and Biochemistry, National Chung Cheng University, Ming Hsiung, Chia Yi 621, Taiwan

Hsiu-Mei Lin, Sheng-Heng Tsai, and Tahsin J. Chow*

Institute of Chemistry, Academia Sinica, Taipei, Taiwan

Received April 5, 2004. Revised Manuscript Received June 2, 2004

Derivatives of 2,3-(1,4-dialkoxyaceno)norbornadiene **1**−**4** underwent ring-opening metathesis polymerization (ROMP) reactions with a ruthenium carbene complex $Cl_2(PCy_3)_2$-Ru=CHPh to afford the corresponding polymers **P1**−**P4** with narrow polydispersity. These materials exhibited luminescence both in solution and as films, whereas **P3** and **P4** were used successfully for the fabrication of light emitting diodes (LED). The device ITO/**P4**/Ca/Al, made of a spin-coated layer of **P3** or **P4**, displayed white light that can be turned on at 7 V with a maximum intensity of 427 cd/m^2 at 15 V. The white electroluminescence is composed of a blue emission band from the aromatic chromophore and a red component derived from solid aggregates. The performance of devices can be improved by insertion of an additional electron-transporting layer, i.e., 1,3,5-tris(2′-(1′-phenyl-1′-H-benzimidazole)-benzene (TPBI). The device ITO/**P4**/TPBI/Mg:Ag displayed blue light with a turn-on voltage of 5 V and maximal intensity of 930 cd/m^2 at 15 V. The change of chromaticity can be ascribed to a shift of charge recombination sites in the bulk of **P4** film. The phenomenon was verified by adjusting the thickness of TPBI layer, whereas a continuous variation in color was observed upon changing bias.

Introduction

Polymeric materials that exhibit both redox and light-emitting properties are of current interest due to their increasing usefulness in a wide variety of electronic and optoelectronic devices.[1−4] The use of poly(*p*-phenylenevinylene) in the fabrication of light-emitting diodes (LED) signaled a breakthrough for it became possible to produce large and flexible display panels at low cost by the spin-coating technique.[5] Further investigations on new types of materials are still in demand through structural modifications. Ring-opening metathesis polymerization (ROMP)[6,7] of hydroquinone-fused norbornadiene derivatives provided an efficient way for the preparation of polymeric materials.[8,9] In an earlier report we described successful application of ROMP polymer containing dialkoxyanthracene chromophores for the preparation of a white LED device.[10] This material, assembled from a single type of monomers, emitted broad-band electroluminescence covering the whole visible region. To the best of our knowledge, it was the first report on a white-color LED device made of single-component polymeric materials without blending or multilayer fabrication. In this context, we launched a program for systematic analyses on this series of new materials which were derived from dialkoxyacene-fused norbornadienes.

ROMP has been intensively investigated for some time and gradually emerged as a powerful and important process for polymer synthesis.[11] The well-developed molybdenum- and ruthenium-based catalysts have demonstrated remarkable success in synthetic applications with various advantages, including their tolerance toward a large variety of functional groups, regardless

(1) Adachi, C.; Nagai, K.; Tamoto, N. *Appl. Phys. Lett.* **1995**, *7*, 531.
(2) Tang, C. W.; VanSlyke, S. A.; Chen, C. H. *J. Appl. Phys.* **1989**, *65*, 3610.
(3) Ahn, T.; Jang, M. S.; Shim, H. K.; Hwang, D. H.; Zyung, T. *Macromolecules* **1999**, *32*, 3279.
(4) Meng, H.; Huang, W. *J. Org. Chem.* **2000**, *65*, 3894.
(5) Burrougjes, B.; Bradley, D. D. C.; Brown, A. R.; Marks, R. N.; MacKay, K.; Friend, R. H.; Burn, P. L.; Holmes, A. B. *Nature* **1990**, *347*, 539.
(6) (a) Ivin, K. J. *Olefin Metathesis*; Academic Press: London, 1983. (b) Grubbs, R. H.; Tumas, W. *Science* **1989**, *243*, 907. (c) Schrock, R. R. *Acc. Chem. Res.* **1990**, *23*, 158. (d) Buchmeiser, M. R. *Chem. Rev.* **2000**, *100*, 565.
(7) Trnka, T. M.; Grubbs, R. H. *Acc. Chem. Res.* **2001**, *34*, 18.
(8) (a) Swager, T. M.; Rock, M. M.; Grubbs, R. H. *New Polym. Mater.* **1990**, *2*, 1. (b) Rock, M. M.; Swager, T. M.; Grubbs, R. H. *Polym. Prepr.* **1990**, *31*, 384.
(9) Chow, T. J.; Yang, Y. C.; Chiu, N. Y.; Hsu, M. A. *J. Chin. Chem. Soc.* **2001**, *48*, 945.
(10) Tsai, M.-L.; Liu, C.-Y.; Hsu, M.-A.; Chow, T. J. *App. Phys. Lett.* **2003**, *82*, 550.
(11) Fürstner, A. *Angew. Chem., Int. Ed. Engl.* **2000**, *39*, 3012.

10.1021/cm049431x CCC: $27.50
Published on Web 07/20/2004

of any additional cocatalyst, and stability in polar solvents such as water.[7,11,12] Norbornene (bicyclo[2.2.1]-heptene) and 7-oxanorbornene (7-oxabicyclo[2.2.1]heptene) are among the most investigated systems by ROMP.[6,7] However, the analogous norbornadiene derivatives have not been equally well studied.[8,9,13,14] Among the few cases are benzonorbornadiene and their homologues, which were catalyzed by Mo(CHBu^t)(NAr)-(OBu^t)$_2$,[13] $WCl_6/SnPh_4$,[15] and recently the ruthenium carbene catalysts.[8,9]

The synthesis and characterization of the ROMP polymers derived from several 1,4-dialkoxyacenonorbornadienes are described in this report, namely, 1,4-dimethoxybenzonorbornadiene (**1**),[19] 1,4-dimethoxynaphthalenonorbornadiene (**2**),[21] 1,4-dimethoxyanthracenonorbornadiene (**3**),[22] and 1,4-di(2′-ethylhexyl)anthracenonorbornadiene (**4**), using a ruthenium carbene complex $Cl_2(PCy_3)_2Ru{=}CHPh$[16] as catalyst. The electrochemical, thermal, and optical properties of these polymers are analyzed along with the performance of LED devices fabricated by **P3** and **P4**.

Experimental Section

Materials. Ruthenium carbene complex $Cl_2(PCy_3)_2Ru{=}CHPh$ and tris(hydroxymethyl)phosphine were purchased from Strem Chemical Co. Dichloromethane was distilled over calcium hydride and degassed. Tetrahydrofuran was obtained by heating with sodium pellets under reflux for 24 h prior to distillation. Cyclopentadiene was prepared by thermal cracking of the dimer at 160 °C immediately before use.[17] 1,4-Dimethoxybenzonorbornadiene (**1**),[8,19,20] 1,4-dimethoxynaphthalenonorbornadiene (**2**),[8,21] and 1,4-dimethoxyanthracenonorbornadiene (**3**)[18,22,23] were prepared according to literature procedures.

Instrumentation. Melting points were determined on a Thomas-Hoover apparatus and are uncorrected. Infrared (IR) spectra were recorded on a Perkin-Elmer 682 FT-IR spectrophotometer by dispersing samples in KBr disks. ^{1}H and ^{13}C NMR spectra were collected on a Brüker DPX-400 spectrometer using $CDCl_3$ as solvent. Thermogravimetric analysis (TGA) was performed on a Shimadzu TGA-50H analyzer at a heating rate of 10 °C/min under nitrogen flow with a rate of 40 mL/min. Differential scanning calorimetry (DSC) was conducted on a Perkin-Elmer DSC-7 instrument at a heating rate of 50 °C/min under nitrogen flow and within the temperature range of 50 and 300 °C. UV−vis absorption and fluorescence emission spectra were measured on a Cary 3E (Varian) spectrophotometer and a Hitachi F4500 fluorimeter (PMT:R928), respectively, whereas emission quantum yields were measured with reference to 9,10-diphenylanthracene. Gel permeation chromatographs (GPC) were obtained on a system equipped with a Waters model 510 HPLC pump, a Universal Liquid Chromatograph model U6K injector, a column-set composed of WATO 44207-HR0.5, WATO 44225-HR3, WATO 44225-HR4, and WATO 44225-HR5E columns, and a Water 486 Tunable Absorbance UV−vis Detector, utilizing THF as eluent at a flow rate of 1.0 mL/min. The mean values of M_n, M_w, and M_n/M_w were calculated on the basis of a polystyrene calibration with a Millennium 2010 Chromatography Manager. Film thickness was measured by a Veeco Dektak surface profile measuring system.

Device Fabrication. Prepatterned indium tin oxide (ITO) substrates with an effective individual device area of 3.14 mm^2 and sheet resistance of <50 ohms/ mm^2 were cleaned by sonication in a detergent solution for 3 min and then washed with a large amount of doubly distilled water. Further sonication in ethanol for 3 min was done before being blown dry with a stream of nitrogen. The ITO substrates were then treated with oxygen plasma for 1 min before use. Polymer films were spin-coated at 3000 rpm onto the substrate from solutions of the polymer (10 mg) in a mixed solvent of 1,2-dichloroethane (1 mL) and toluene (1 mL). The devices were placed under vacuum (1×10^{-4} Torr) for 12 h to remove residual solvents. A 40 nm cathode layer was deposited by evaporation of Ca at 2×10^{-5} Torr. The device was completed by capping an Al layer with 120 nm thickness.

1,4-Di(2′-ethylhexyl)anthracenonorbornadiene (4). A stirring solution of 1,4-anthraquinonorbornadiene[22,23] (1.6 g, 6.0 mmol) and Cs_2CO_3 in DMF (10 mL) was stirred and heated 100 °C for 30 min. To the solution was then added an excess amount of 2-ethylhexyl bromide, and the mixture was heated for an additional 10 h. Most of the solvent was removed, and the resulting residue was mixed with CH_2Cl_2 (10 mL) and *n*-hexane (100 mL) and cooled with an ice−water bath to precipitate inorganic material. After suction filtration through a pad of silica gel, the solvent was evaporated to leave crude **4** as a viscous oil (2.8 g, 96%): IR (KBr, cm^{-1}) 1659, 1456, 1323, 1023, 894. ^{1}H NMR ($CDCl_3$, 300 MHz) δ 8.56 (d, J = 2.4 Hz, 2H), 7.94−7.97 (m, 2H), 7.37−739 (m, 2H), 6.71 (m, 2H), 4.29 (br, 2H), 4.07 (dd, J = 6.5, 3.9 Hz, 2H), 3.99 (dd, J = 6.5, 3.9 Hz, 2H), 2.23 (d, J = 7.6 Hz, 1H), 2.16 (d, J = 7.6 Hz, 1H), 1.56−1.86 (m, 10 H), 1.42−1.43 (m, 8H), 1.04−1.06 (m, 6H), 0.97−1.02 (m, 6H). ^{13}C NMR ($CDCl_3$, 75.5 MHz) δ 143.8, 140.9, 133.2, 131.3, 128.3, 127.7, 125.0, 120.7, 62.9, 46.7, 40.8, 30.7, 29.3, 24.0, 23.2, 14.2, 11.4. HRMS: calcd for $C_{35}H_{46}O_2$, 498.3498; found, 498.3500.

General Procedure for Ring-Opening Polymerization. Into a stirred solution of monomer (**1**−**4**) in CH_2Cl_2 (concentrated 0.4 M) under a nitrogen atmosphere was added ruthenium carbene complex $Cl_2(PCy_3)_2Ru{=}CHPh$ (4 mol %).[24] The reaction mixture was stirred at room temperature until monomer was not detected by TLC analysis (12 h). To the solution was added ethyl vinyl ether (10−20 equiv) to terminate polymerization. The resulting brown reaction mixture was filtered through a pad of silica gel into a beaker containing hexane. The solid thus precipitated was collected and washed 3 times with hexane to give an off-white polymeric material. The polymeric material thereby obtained was further purified by dissolving in CH_2Cl_2 and stirring with silica gel containing triethylamine (2 equiv) and tris(hydroxymethyl)phosphine (86 equiv) for 30 min. It was then filtered and dried in vacuo to yield polymers **P1** (75%), **P2** (80%), **P3** (83%), and **P4** (80%). The IR, ^{1}H NMR, and ^{13}C NMR spectral data are given below.

Physical data of **P1**: IR (KBr, cm^{-1}) 1603, 1498, 1258. ^{1}H NMR ($CDCl_3$, 400 MHz) δ 6.55−6.65 (m, 2H), 5.48−5.51 (m, 2H, −C*H*=C*H*−), 4.26 (br, 1.6H, *H*C−CH=CH−), 3.62−3.73 (m, 6.4H, *H*C−CH=CH− and −OC*H*$_3$), 2.70 (br, 1H, −HC*H*−), 1.77 (br, 1H, −*H*CH−). ^{13}C NMR ($CDCl_3$, 100 MHz) δ151.5, 151.2, 135.8, 136.6, 133.4, 132.9, 132.4, 110.4, 110.2, 56.4, 56.2, 46.5, 45.9, 42.5, 41.9, 41.7, 41.6.

Physical data of **P2**: IR (KBr, cm^{-1}) 1636, 1599, 1461, 1259. ^{1}H NMR ($CDCl_3$, 400 MHz) δ 8.03 (br, 2H), 7.21−7.36 (m, 2H), 5.75 (br, 2H, −C*H*=C*H*−), 4.46 (br, 1.3H, *H*C−CH=CH−),

(12) Lynn, D. M.; Mohr, B.; Grubbs, R. H.; Henling, L. M.; Day, M. W. *J. Am. Chem. Soc.* **2000**, *122*, 6601.
(13) Moore, J. S. In *Comprehensive Organometallic Chemistry II*; Hegedus, L. S., Ed.; Pergamon Press: Urbana, 1995; Vol. 12, p 1209.
(14) Gillan, E. M. D.; Hamilton, J. G.; Mackey, O. N. D.; Rooney, J. J. *J. Mol. Catal.* **1988**, *46*, 359.
(15) El-Saafin, I. F. A. F.; Feast, W. J. *J. Mol. Catal.* **1982**, *15*, 61.
(16) Nguyen, S. T.; Grubbs, R. H.; Ziller, J. W. *J. Am. Chem. Soc.* **1993**, *115*, 9858.
(17) Moffett, R. B. *Organic Synthesis*; John Wiley & Sons: New York, 1963, Collect. Vol. 4, pp 238−241.
(18) Patney, H. K.; Paddon-Row, M. N. *Synthesis* **1986**, 326.
(19) Marchand, A. P.; Allen, R. W. *J. Org. Chem.* **1974**, *39*, 1596.
(20) Meinwald, J.; Wiley, G. A. *J. Am. Chem. Soc.* **1958**, *80*, 3667.
(21) Paquette, L. A.; Bellamy, F.; Böhm, M. C.; Gleiter, R. *J. Org. Chem.* **1980**, *45*, 4913.
(22) Kumar, K.; Tepper, R. J.; Zeng, Y.; Zimmt, M. B. *J. Org. Chem.* **1995**, *60*, 4051.
(23) Majumdar, G.; Murty, K. V. S. N.; Mal, D. *Tetrahedron Lett.* **1994**, *35*, 6139.
(24) Grubbs, R. H.; Maynard, H. D. *Tetrahedron Lett.* **1999**, *40*, 4137.

Scheme 1

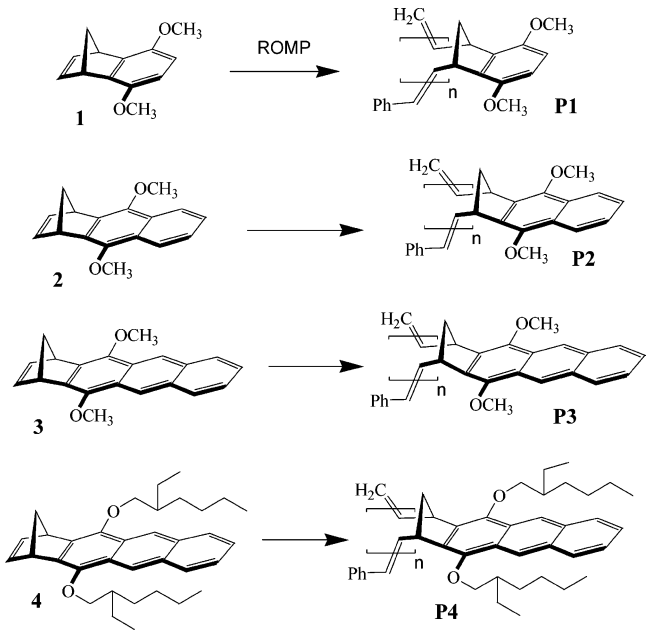

3.60−4.15 (m, 6.7H, *H*C−CH=CH− and −OC*H*$_3$), 2.67 (br, 1H, −HC*H*−), 1.85 (br, 1H, −*H*CH−). ^{13}C NMR ($CDCl_3$, 100 MHz) δ 148.4, 135.8, 134.9, 134.2, 132.8, 132.0, 130.0, 125,2, 122.1, 61.8, 60.9, 46.5, 45.7, 45.4, 43.7, 42.7, 42.3, 41.1, 40.9.

Physical data of **P3**: IR (KBr, cm^{-1}) 1636, 1456, 1336. ^{1}H NMR ($CDCl_3$, 400 MHz) δ 8.53 (br, 2H), 7.81 (br, 2H), 7.00−7.35 (m, 2H), 5.75 (br, 2H, −C*H*=C*H*−), 4.39 (br, 1H, *H*C−CH=CH−), 3.49−4.12 (m, 7H, *H*C−CH=CH− and −OC*H*$_3$), 2.50 (br, 1H, −HC*H*−), 1.85 (br, 1H, −*H*CH−). ^{13}C NMR ($CDCl_3$, 100 MHz) δ 148.5, 148.1, 134.6, 132.9, 132.2, 131.6, 131.2, 129.3, 128.4, 126.6, 126.2, 125.3, 120.9, 61.9, 61.1, 46.1, 45.5, 44.0, 42.9, 41.1.

Physical data of **P4**: IR (KBr, cm^{-1}) 1629, 1449, 1379, 1327. ^{1}H NMR ($CDCl_3$, 300 MHz) δ 8.57 (br, 2H), 7.86 (br, 2H), 7.00−7.31 (m, 2H), 5.95 (br, 2H, −C*H*=C*H*−), 3.50−4.80 (m, 8H, *H*C−CH=CH− and −OC*H*$_2$), 2.90 (br, 2H, −HC*H*−), 2.05 (br, 1H, −*H*CH−), 0.68−1.80 (m, 26H). ^{13}C NMR ($CDCl_3$, 125 MHz) δ 147.0, 134.3, 132.8, 131.0, 128.5, 124.9, 120.8, 45.7, 42.0, 41.0, 30.3, 29.1, 23.7, 23.0, 14.0, 11.2.

Results and Discussion

Structural Elucidation. Polymers **P1**, **P2**, **P3**, and **P4** were synthesized by ROMP reactions using $Cl_2(PCy_3)_2Ru$=CHPh (4 mol %) as catalyst (Scheme 1).[25] The chemical structures of polymers **P1**, **P2**, **P3**, and **P4** were confirmed by ^{1}H and ^{13}C NMR spectral analyses. Diagnostic differences in the ^{1}H NMR signals of the methylene and vinylic protons of polymers were observed comparing to those of the monomers. In the monomers the two magnetically nonequivalent protons on the methano bridge appeared at δ 2.26/2.29 for **1**, 2.24/2.34 for **2**, 2.20/2.29 for **3**, and 2.15/2.22 for **4** with a difference of less than 0.1 ppm. However, the methylene protons in the polymers gave two broad signals appearing at δ 1.77/2.70, 1.86/2.67, 1.85/ 2.50, and 2.15/2.90 for **P1**, **P2**, **P3**, and **P4**, respectively. The methylene protons in the polymers exhibit larger differences (0.6−0.9 ppm) in chemical shifts, which indicates that the anisotropic shielding environment experienced by the methylene protons becomes greater as a result of ring opening. The resonance signals for the vinylic protons in the polymers of norbornene and norbornadiene derivatives are shifted upfield and appear as two discernible signals at δ 5.7 and δ 5.5 due to the trans and cis geometrical isomers.[25] In the present study, however, an unresolved broad signal was displayed by the vinylic protons of all polymers **P1**, **P2**, **P3**, and **P4** at δ 5.51, 5.75, 5.75, and 5.95, respectively. The ^{1}H NMR spectra of monomer **4** and its corresponding polymer **P4** showed additional signals at higher field (δ 0.9−1.8 and 3.9−4.3) due to the absorption of 2-ethylhexyl side chains.

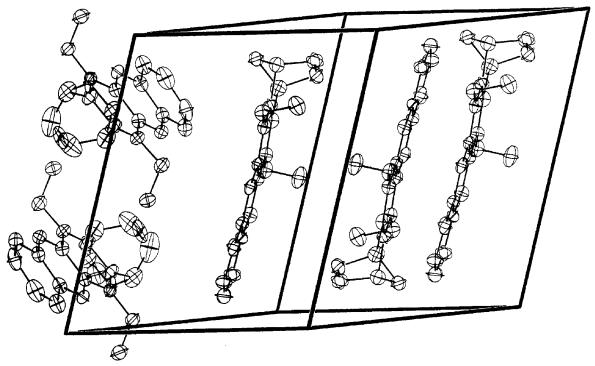

Figure 1. Unit cell in the crystal of compound **3** showing the stacking pattern of molecules. There are two conformational isomers coexisting in a single crystal. The *transoid* isomers (orientation of the two methoxy groups) are stacked along the *b* axis (structures on the left side). Disorder on the [2.2.1] ring moieties are observed. The *cisoid* isomers are packed in a nearly perpendicular orientation to the *transoid* isomers as shown on the right side.

The ^{13}C NMR spectrum of the polymers showed more resonance signals than the number of peaks expected if symmetrical structures are adapted. This is caused by the complexity of microstructures existing in the polymers, such as trans/cis geometry and ring tacticity. The microstructure of the polymers made from norbornenes and norbornadienes by ROMP have been examined in considerable detail using ^{13}C NMR spectroscopy.[26] However, the distribution of trans and cis double bonds in the present polymers could not be properly determined because the ^{13}C NMR signals were not well resolved.

The crystal structure of compound **3** was solved by X-ray diffraction analysis, and the stacking pattern in a unit cell is shown in Figure 1. There are two conformers coexisting in a single crystal as a result of flexible rotation of the methoxy groups. The $\pi-\pi$ stacking, which was expected among anthracene moieties, was not apparent. In polymeric structures, e.g., **P3** and **P4**, the aromatic chromophores may form aggregates at local regions. Such aggregations are believed to be responsible for the observation of a red-shifted luminescence.[27−29] The origin of these aggregates, e.g., whether they were derived from complicated $\pi-\pi$ interactions or not, is not fully understood yet.

(25) Asrar, J. *Macromolecules* **1992**, *25*, 5150.

(26) Fawcett, A. H.; Hamilton, J. G.; Rooney, J. J. In *Polymer Spectroscopy*; Fawcett, A. H., Ed.; John Wiley & Sons: Chichester, 1996; pp 30−52.

(27) Chang, R.; Hsu, J. H.; Fann, W. S.; Yu, J.; Lin, S. H.; Lee, Y. Z.; Chen, S. A. *Chem. Phys. Lett.* **2000**, *317*, 153.

(28) Witten, D. G. *Acc. Chem. Res.* **1993**, *26*, 502.

Table 1. Ring-Opening Metathesis Polymerization of 1,4-Dialkoxylacenonorbornadienes 1, 2, 3, and 4[a]

entry	polymers	[M]/[C]	yield (%)	$10^{-3}\,M_n$ [b]	$10^{-3}\,M_w$ [b]	PDI[c]
1	P1	25	75	4.85	5.15	1.05
2		50	78	7.21	8.12	1.12
3		100	69	14.33	16.21	1.13
4		200	96	29.00	35.85	1.23
5	P2	25	80	6.81	7.13	1.04
6		50	81	7.01	8.60	1.22
7		100	67	19.60	21.77	1.11
8		200	94	23.46	29.15	1.24
9	P3	25	83	4.99	5.32	1.06
10		50	86	9.19	11.13	1.21
11		100	93	9.83	17.31	1.76
12		200	94	7.19	18.46	2.57
13	P4	25		5.59	5.89	1.05
14		25[d]		4.70	5.09	1.08
15		25[e]		4.20	4.66	1.11

[a] Polymerizations were run in dichloromethane ([M] = 0.4 M) at room temperature under a nitrogen atmosphere with ruthenium catalyst for 12 h. [b] Molecular weight (M_w) and the number-average molecular weight (M_n) were determined by GPC using polystyrene standards. [c] PDI = molecular weight distribution (MWD) = M_w/M_n. [d] Polymerization was performed at 0 °C. [e] Polymerization was conducted at −45 °C.

Molecular Weights. The molecular weights of the polymers were measured by GPC analysis using THF as the eluent against polystyrene standards and are summarized in Table 1. We first examined the polymeric products that were obtained from the ROMP reactions performed in CH_2Cl_2 (concentration of monomer = 0.4 M) at room temperature using the ruthenium complex (monomer-to-catalyst molar ratio: [M]/[C] = 25:1). As shown in Table 1, entries 1, 5, and 9, polymerization of **1**, **2**, and **3** proceeded in good yields. The number-average molecular weights (M_n) of polymers **P1**, **P2**, and **P3** were measured as 4850, 6810, and 4990, respectively, with narrow polydispersity (PDI = 1.04−1.06). The molecular weights (M_w and M_n) of polymer and the PDI were not very sensitive to the change of temperature, as indicated by the polymerization of **2** at lower temperatures (entries 5, 13, 14, and 15). The effect of the monomer-to-catalyst molar ratio ([M]/[C]) on ROMP was then investigated for all monomers. A good linear relationship between the molecular weight (both M_w and M_n) of polymers and the [M]/[C] ratios could be correlated for the polymerization of **1** (entries 1−4). As the monomer becomes bulkier, deviation from a linear relationship becomes perceivable. For the polymerization of monomer **2** (entries 5−8), the molecular weight of polymer increased as the quantity of catalyst decreased, with the PDI still being narrow. However, for the most bulky monomer **3** to **P3** shown in entries 9−12, a poor linear relationship was observed between molecular weight and [M]/[C], along with a substantial increase of PDI. Also observed for **P3** were higher yields along with a significant reduction in the molecular weights compared with those of **P1** and **P2**.

Thermal Properties. The thermal properties of polymers **P1**, **P2**, and **P3** were evaluated by means of TGA and DSC under nitrogen atmosphere, and the results are summarized in Table 2. The thermograms revealed that all polymers exhibited good thermal stability up to 200 °C, and the temperature for 10% weight loss was 354, 370, and 420 °C for **P1**, **P2**, and **P3**, respectively. Thermal analysis by DSC indicated that the glass-transition temperature (T_g) was 159, 206, and >300 °C for **P1**, **P2**, and **P3**, respectively. It is well-known that increasing the molecular weight of the polymer and incorporation of bulky groups into the polymer backbone can elevate the T_g of the polymer, because the increased rigidity reduced the mobility of polymeric chains. Polymer **P3** exhibited the highest T_g, although having a lower molecular weight than both **P1** and **P2**, suggesting that the chain motion in **P3** was strongly restrained due to the bulky 1,4-dimethoxy-anthracenyl group. Polymers **P1**, **P2**, and **P3** did not show a crystalline melting point (T_m) up to 300 °C, indicating the polymers were amorphous in nature.

Table 2. Thermal and Optical Properties for Polymers P1, P2, P3, and P4 Compared with the Corresponding Monomers

	TGA, $T_{-10\%}$ (°C)[a]	DAC, T_g (°C)	UV−vis, λ_{max} (nm)[b,c]	fluorescence λ_{em} (nm) in CH_2Cl_2 [d]	fluorescence λ_{em} (nm) solid film
P1	354	159	232/288	316 (0.01)	345
1			233/296	335 (0.02)	333
P2	370	206	240/296	393 (0.42)	385
2			246/289	365 (0.43)	354
P3	420	>300	268/377	481 (0.12)	450
3			271/360	463 (0.53)	439
P4		>300	273/382	482 (0.09)	470
4			273/368	471 (0.54)	469

[a] $T_{-10\%}$ is the 10% weight loss temperature of polymers determined by TGA. [b] Spectra taken in dichloromethane. [c] Peak maximum for the two major absorption bands. [d] Quantum yields are listed in the blankets using 9,10-diphenylanthracene as standard.

Optical Properties. The UV absorption and fluorescence spectroscopic properties of the polymers and their corresponding monomers were investigated in CH_2Cl_2 solution. Table 2 summarizes the UV absorption and fluorescence spectral data of the polymers and monomers. The profiles of the UV absorption spectra for the polymers are similar to their corresponding monomers. As expected, the maximum UV absorption wavelengths (λ_{max}) increase systematically with the increasing number of fused phenyl rings.

All monomers and the respective polymers exhibit two major absorption bands, which correspond to the ^1L_a and ^1L_b transitions of benzene. The ones at longer wavelengths appeared at λ_{max} 296, 289, 360, and 368 nm, respectively, for compounds **1**, **2**, **3**, and **4** (Table 2). Those of polymers **P2**, **P3**, and **P4** show slight red shifts compared to the monomers, i.e., at 296, 377, and 382 nm. The absorption band of **P1** looks somewhat abnormal (at 288 nm) since it shows a mild blue shift with respect to that of **1**. The phenomenon can be explained by the presence of a pronounced transannular orbital interaction between the two π-systems across the bicyclic skeleton. It was well understood that the two sets of π-bonds of norbornadiene overlap with each other through space, which may induce an observable change on their electronic structures.[30] Such interaction is expected to be stronger in **1**, due to the closeness in energy between the interacting π-systems, than those

(29) Mataka, S.; Shigaki, K.; Sawada, T.; Mitoma, Y.; Taniguchi, M.; Thiemann, T.; Ohga, K.; Egashira, N. *Angew. Chem., Int. Ed. Engl.* **1998**, *37*, 2532.

(30) Scholes, G. D.; Ghiggino, K. P.; Oliver, A. M.; Paddon-Row, M. N. *J. Am. Chem. Soc.* **1993**, *115*, 4345.

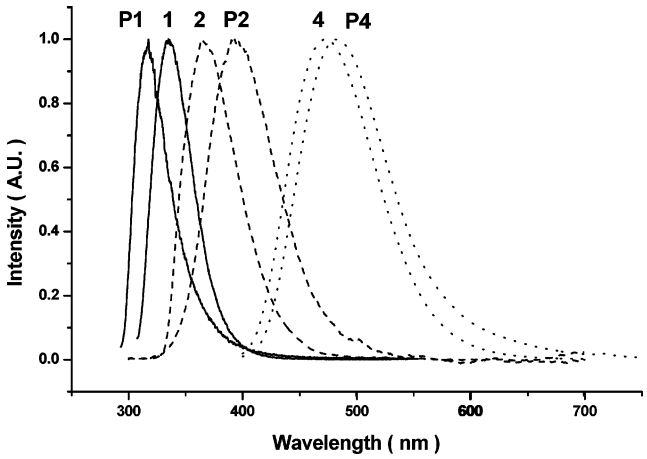

Figure 2. Normalized photoluminescence of monomers **1**, **2**, and **4** and polymers **P1**, **P2**, and **P4** in CH_2Cl_2. The spectra of **3** and **P3** are similar to those of **4** and **P4**.

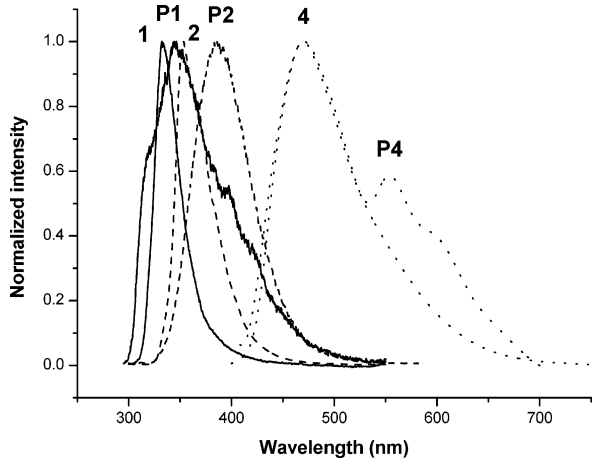

Figure 3. Normalized photoluminescence of monomers **1**, **2**, and **4** and polymers **P1**, **P2**, and **P4** in the solid state. Peak broadening is apparent for polymers, whereas in the emission of **P4** low-energy sidebands can be clearly identified.

in **2**−**4**. Ring opening of **1** to **P1** released the ring strain and therefore weakened the $\pi-\pi$ interaction. Reduction of the potential energy of the π-electrons in the ground state resulted in a blue shift of the absorption transitions.

Excitation on the ^1L_a bands of all polymers and monomers induced luminescence in various quantum yields. Their fluorescence spectra are shown in Figure 2 and emission maxima in Table 2. The fluorescence spectra of polymers **P2** (393 nm), **P3** (481 nm), and **P4** (482 nm) in CH_2Cl_2 exhibit red shifts with respect to their monomers, except that of **P1** (316 nm) exhibits a blue shift in line with the blue shift of absorptions. Also presented in Table 2 are the emission maxima of compounds in their solid state. Since in LED devices the emitting materials are fabricated in films, it is important to realize their luminescence properties in the solid state. For comparison purposes, the emission spectra of both the monomers and polymers are shown in Figure 3, and the peak maxima (λ_{em}) are listed in Table 2. As a general phenomenon, all emissions in the solid state showed some degree of blue shifts compared to those in solution (e.g., CH_2Cl_2). The bandwidths of monomers **1** and **2** are appreciably narrowed (cf. the corresponding bands in Figures 2 and 3), which can be

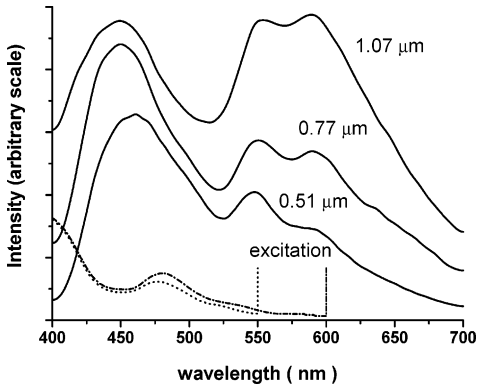

Figure 4. (Upper curves) Emission spectra of **P4** films of various thickness (solid lines): top curve, 1.07 μm; middle curve, 0.77 μm; bottom curve, 0.51 μm. (Lower curves) Photoexcitation spectra of **P4** film (dotted and dash−dotted lines), monitored at two different wavelengths (vertical lines at 550 and 600 nm). Both spectra exhibit the presence of a new broad band centered at 480 nm, which was absent in the absorption spectrum of **P4** in dilute solutions. This band was believed to come from solid aggregates in the films.

ascribed to the restriction on molecular motions in the solid state. It is also observed in Figure 3 that the emission bandwidths of polymers are considerably broader than those of monomers, whereas new emission bands appeared on the low-energy sides.

The origin of these low-energy bands is not fully clear yet. A plausible explanation for the new emitting species is due to the formation of aggregates in the solid state.[27−29,32] Further analyses on the effect of film thickness revealed that the relative emission intensity of these new bands changed with thickness. As shown in Figure 4, the red emitting component of **P4** films became more intense while the film thickness was increased from 0.51 to 0.77 and 1.07 μm. The aggregates were more abundant inside the bulk of the film as compared with the region near the surface. Photoexcitation spectra monitored at two different wavelengths (550 and 600 nm) exhibit a new absorption at ca. 480 nm, which was not seen in dilute solutions. The formation of aggregates therefore was evidenced by a distinctive absorption band.

Redox Properties. All monomers **1**−**4** exhibit reversible oxidative waves in cyclic voltammetry (CV). The onset of their oxidation potentials (rather than the half-wave potentials) are listed in Table 3. To use the polymeric materials on photoelectric devices, it is necessary to know the redox property of films. Therefore, thin films of **P1**−**P4** were coated onto the surface of a platinum working electrode and their oxidative potentials were measured in CH_3CN. They all showed irreversible oxidation waves at ca. 0.75−0.95 V which were not significantly different form those measured in CH_2Cl_2 solution. From these data the ionization potential (I_p) (or HOMO) can be deduced by the equation $I_p = E_{ox} + 4.40$ eV,[31] where E_{ox} is the onset of peaks. Since it is not feasible to measure the reduction potentials directly by CV, the values of their electron affinity (E_a) (or LUMO) can be deduced by the difference of I_p and

(31) Janietz, S.; Bradley, D. D. C.; Grell, M.; Giebeler, C.; Indasekaran, M.; Woo, E. P. *Appl. Phys. Lett.* **1998**, *73*, 2453.
(32) (a) Shi, S.; Liu, J.; Yang, Y. *J. Appl. Phys.* **2000**, *87*, 4254. (b) He, G.; Li, Y.; Liu, J.; Yang, Y. *Appl. Phys. Lett.* **2002**, *80*, 4247.

Table 3. Estimated Ionization Potential (I_p), Electron Affinity (E_a), and Band 0−0 Absorption Energy (λ_{0-0}) of Polymers and Monomers

	1	P1	2	P2	3	P3	4	P4
E_{ox} (eV)	1.24[a]	0.92[b]	1.10[a]	0.78[b]	0.93[a]	0.72[b]	0.87[a]	0.78[b]
λ_{0-0}[c] (nm) (eV)	318 (3.90)	305 (4.06)	330 (3.76)	327 (3.79)	400 (3.10)	410 (3.02)	400 (3.10)	410 (3.02)
I_p[d] (eV)	5.64	5.32	5.50	5.18	5.33	5.12	5.27	5.18
E_a[e] (eV)	1.74	1.26	1.74	1.39	2.23	2.10	2.17	2.16

[a] Measured at the onset of oxidation waves in CH_2Cl_2. [b] Onset of oxidation waves of films in CH_3CN. [c] The edge (λ_{0-0}) of absorption bands. [d] $I_p = E_{ox} + 4.4$ (ref 1a). [e] $E_a = I_p - E_{0-0}$.

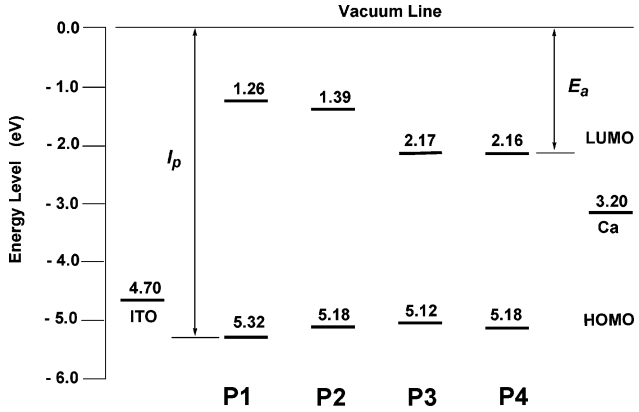

Figure 5. Energy profile for polymers **P1**−**P4**, where the ionization potential I_p corresponds to the energy of the highest occupied molecular orbital (HOMO) and electron affinity E_a to the energy of lowest unoccupied molecular orbital (LUMO). The work functions of calcium and ITO glass are marked for comparison.

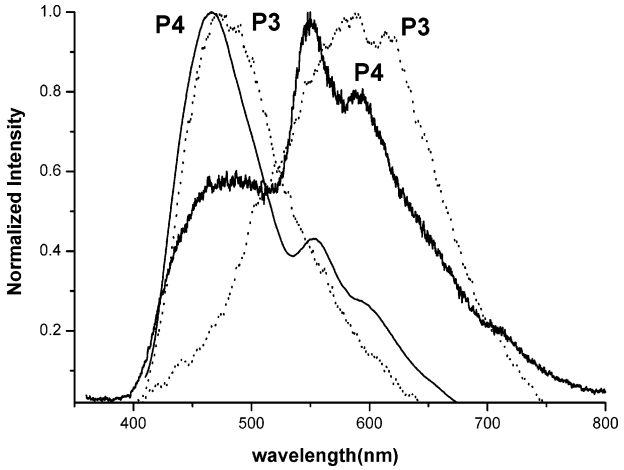

Figure 6. Normalized photoluminescence (left) and electroluminescence (right) of polymer films **P3** (· · ·) and **P4** (—). The electroluminescence was emitted from single-layer device ITO/polymer/Ca/Al. Polymer films were formed by spin coating a solution of the respective polymers in 1,2-dichloroethane.

the absorption energy of the 0−0 transition (λ_{0-0}). The band gap values were taken from the absorption edges of each spectrum.

An energy profile is constructed in Figure 5 for the polymers. The HOMO and LUMO levels of **P3** and **P4** are comparable to the work function of calcium and ITO glass and therefore are considered suitable for the fabrication of light-emitting diodes (LED). The emissions of **P1** and **P2** are confined in the UV region; also because their LUMO levels are much higher than the work function of calcium, these two materials were not suitable for LED fabrication.

Single-Layer LED Devices. The luminescence quantum yields of **P3** and **P4** are substantially lower than those of their monomer precursors (Table 2). There are many possible reasons for it, such as self-quenching due to microcrystallization in solid. The introduction of more flexible 2-ethylhexyl side chains in **P4** is designed in order to enhance amorphous morphology and therefore to reduce the degree of self-quenching. The result was rather unexpected, however; in addition to promoting the emission quantum yield of acenes, the low-energy bands deriving from aggregates (λ_{em} at 555 and 600 nm) were also promoted significantly.

The films of **P3** and **P4** were prepared by spin coating; then the films were sandwiched between two conducting electrodes for preliminary examination. In a typical procedure, a solution of polymer (**P3** or **P4**) in 1,2-dichloroethane (1 wt %) was spin coated (3000 rpm) onto a pretreated ITO glass, which was then dried in a vacuum chamber (10−5 Torr) to form a solid film about 40 nm thick. A layer of calcium (30 nm) was deposited on top of the film by vapor deposition, followed by an aluminum capping (120 nm) to completion. Both devices (**P3** and **P4**) can be turned on at 8 V, surprisingly, in white light. So far as we know, this is the first example of observing white-light emission from a single-component polymer without blending of multiple chromophores.

In Figure 6 the spectra of emissions from devices ITO/polymer/Ca/Al were shown. The photoluminescence of films **P3** and **P4** both exhibit blue color originating from dialkoxyanthracene. The minor red-colored component of the photoluminescence (PL) became much more intense in the spectra of electroluminescence (EL). A combination of both blue and red components yielded a white emission covering the full range of the visible region. The brightness of these emissions, however, was rather low even under high voltage, e.g., 15 cd/m^2 at 18 V for **P3** and 137 cd/m^2 at 17 V for **P4**.

Film Morphology. After several preliminary examinations it was clear that the devices fabricated using **P4** worked better than those of **P3**. The presence of flexible 2-ethylhexyl side chains in **P4** must have a positive effect of promoting the homogeneity of the films. The net emission spectrum is the combination of a blue component deriving from the original anthracene chromophore and a red component deriving from aggregates.

The chromaticity of color can be tuned slightly by adjusting the relative intensities of the blue and red components. It was found that solvents, which were used for spin coating, showed an observable influence on emission spectra. Films prepared from solutions of **P4** in both toluene and cyclohexane emit white light of better chromaticity than that made from 1,2-dichloroethane. The effect of solvent on emission can be seen in Figure 7, whereas the films of **P4** were prepared either from single solvents, e.g., toluene and cyclohexane, or from mixtures of solvents, e.g., toluene/1,2-dichloroethane (6:4) and toluene/cyclohexane (6:4). Despite some

Table 4. Device Performance for the Single-Layer Device ITO/P4/Ca/Al Using Different Solvents for Spin Casting the Films[a]

ITO/**P4**/Ca/Al solvent for spin coating	turn-on voltage	luminance (cd/m^2)	current density (mA/cm^2)	max. quantum efficiency
toluene	6.5 V	427 at 15 V	330 at 15 V	0.084%
1,2-dichloroethane (DCE)	8 V	105 at 15 V	480 at 15 V	0.013%
cyclohexane	11.5 V	23 at 17 V	102 at 17 V	0.008%
toluene/DCE (6:4)	7 V	35 at 13 V	115 at 13 V	0.009%
toluene/cyclohexane (6:4)	8.5 V	112 at 19 V	105 at 19 V	0.086%

[a] The corresponding spectra are shown in Figures 6 and 7.

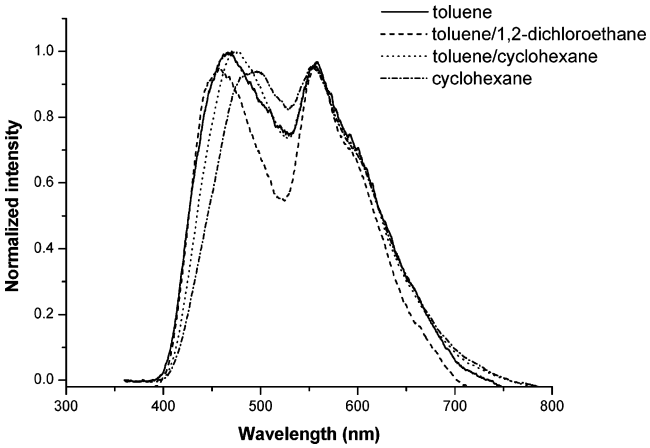

Figure 7. Emission spectra of the device ITO/**P4**/Ca/Al in which the emitting film was prepared by spin-coating a solution of **P4** in different solvents. Solvents influence film morphology, so as to the emission spectra.

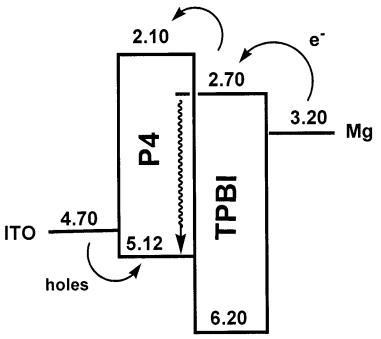

Figure 8. Energy profile for a double-layer device ITO/**P4**/TPBI/Mg in which TPBI acted as electron transporter as well as hole blocker.

minor variations on spectral patterns, all emissions appeared as broad bands covering the complete visible range, i.e., 400−700 nm. A comparison of device performance is given in Table 4, from which toluene seems to be the most suitable medium for the purpose of spin coating.

Device Optimization. From the energy profile in Figure 5 it seems that an energy gap exists between the LUMO (−2.10 V) level of **P4** and the work function of calcium (−3.20 V). To enhance the electron mobility it may be helpful to add a layer of electron transporter between the electrode and polymer film. TPBI (1,3,5-tris(2′-(1′-phenyl-1′-*H*-benzimidazole)benzene) is a widely used electron-transporting material which has a relatively low LUMO level (−2.70 V). It can also act as a hole blocker, since its low HOMO level (−6.2 V) can prevent positive holes from migrating across the films interface. To improve electron transport, a layer of TPBI was inserted into the device as shown in Figure 8.

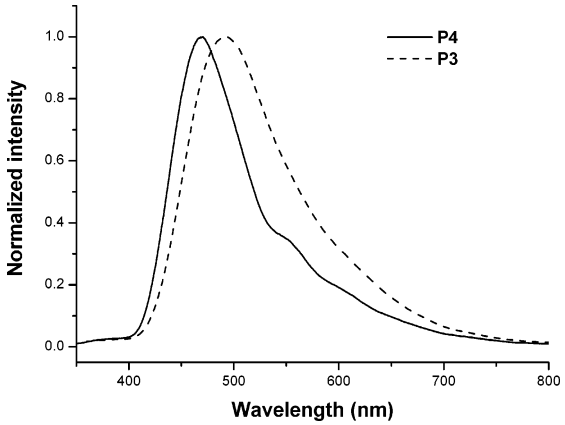

Figure 9. Electroluminescence spectra of the double-layer devices ITO/polymer/TPBI/Mg:Ag using **P3** (· · ·) and **P4** (—) as emitting materials.

Double-layer devices with configuration ITO/polymer/TPBI/Mg:Ag were fabricated by spin-coating films of the polymer (**P3** or **P4)** onto a pretreated surface of ITO glasses in a similar way as before. The polymer film was covered by a thin layer of TPBI (40 nm thickness) through vapor deposition in a vacuum chamber. The combined organic layers were coated by coevaporating a Mg−Ag (10:1) alloy; then the device was completed by capping with pure silver as anode.

The double-layer devices indeed performed better than the one made of a single layer. Both devices made of **P3** and **P4** can be turned on at ca. 5 V. The maximum brightness of the device using **P4** was 930 cd/m^2 at 15 V, and that of **P3** was 285 cd/ m^2. The external quantum efficiency of **P4** increased to 0.34%, compared to 0.084% for the single-layer one (Table 4). However, the spectra of these devices exhibited normal blue emission similar to their photoluminescence, i.e., without much of the red components from aggregates (Figure 9). This phenomenon may be explained by the change of position for charge recombination. In double-layer devices, the migration of holes was stopped at the interface between polymer and TPBI, where charge recombination appeared most efficiently. At the layer interface, the concentration of aggregates is relatively low. However, in single-layer devices, charge recombination proceeds most likely inside the bulk of polymeric materials, where aggregates scattered around in close proximities allow efficient Förster-type energy transfers.

From Blue to White. All the LED devices, so far described, are luminescent with stable spectra independent of applied voltage. The intensity of light increases with increasing voltage, yet the spectrum stays invariant. If the distribution of blue and red components in the materials is not the same at the surface as inside the medium, then it is possible to change color by shifting the position of the charge recombination. The

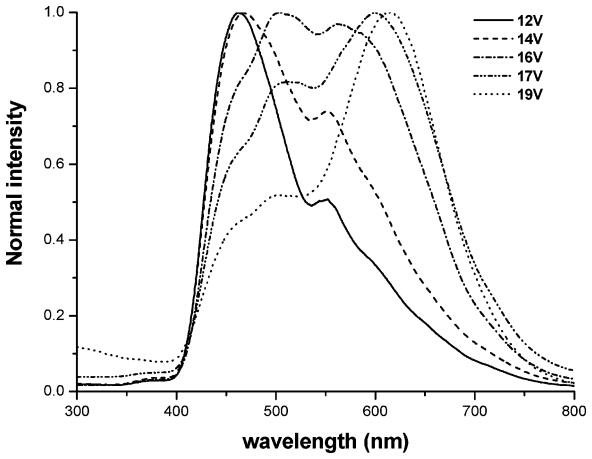

Figure 10. Electroluminescence spectra of device ITO/**P4** (40 nm)/TPBI (10 nm)/ Mg:Ag at different voltages. The change in chromaticity with applied bias was caused by a shift of the charge recombination site.

aggregates of chromophores, which are responsible for the red emission, seem to be more abundant inside the medium than on the surface (or at the interface region) of polymer films. For double-layer device ITO/**P4**/TPBI/ Mg:Ag, if the site of charge recombination can be shifted away from the interface of **P4**/TPBI toward the center of **P4** film, the color of the device should be turned to be more reddish.

The hypothesis can be verified by either increasing the speed of electrons or reducing the speed of holes. In either way the site of charge recombination should be shifted to the left side of the **P4**/TPBI interface according to the plot in Figure 8. Therefore, a new device was fabricated following the same process except the thickness of TPBI was reduced to 10 nm rather than the usual 40 nm. Electrons coming cathode should now migrate more readily through the TPBI interface into **P4**. At low voltage (<12 V) this device displayed a spectrum similar to the PL of **P4** (cf. Figures 9 and 10). When the applied bias increased, the red emission (from aggregates) gradually became more intense. At voltages greater than 16 V, the color of the device became white as in single-layer devices. At high voltage a greater amount of electrons migrate across the thin film of TPBI into the bulk of **P4**, where they recombined with holes to emit red light. A continuous plot on spectral changes is shown in Figure 10.

Summary

Polymers prepared from dialkoxyacene-substituted norbornadienes by ROMP emit luminescence containing a major component from the normal emission of aromatic chromophores and a minor component from aggregates. In the visible region the normal emissions of **P3** and **P4** constitute the blue emission, whereas those from aggregates exhibit red color. An effective LED device can be assembled by sandwiching a single film of either **P3** or **P4** between the electrodes of ITO and calcium. Such devices displayed white light as a result of combining the normal blue emission and an intensified red emission. The chromaticity of the devices changed slightly with solvents used for spin coating due to the change of film morphology. The spectrum of white color stayed invariant, however, upon changing bias.

The quantum yield of devices can be improved by inserting a layer of TPBI between **P4** and calcium in order to improve electron transport. A typical device ITO/**P4**/TPBI/Mg:Ag can be turned on at 5 V with external quantum efficiency 0.34%, which exhibits a maximum light intensity of 930 cd/m^2 at 15 V. The emission color is blue, similar to the photoluminescence of **P4** film. The change of color can be ascribed to a shift of charge recombination sites toward the interface of **P4** and TPBI. At the interface the concentration of aggregates is less abundant than that inside the bulk of the emitting material, so the red emission became less intense. This hypothesis can be verified by reducing the thickness of TPBI in the devices. In such devices at higher voltages, electrons pass faster through the layer of TPBI and annihilate with holes inside the medium of **P4**. The color of devices therefore can be tuned gradually from blue to white upon increasing the applied bias.

Acknowledgment. Financial support from the National Science Council of the Republic of China is gratefully acknowledged. We are grateful to Professor Yen-Nan Chang for helpful discussions on the crystal structure.

Supporting Information Available: X-ray crystallographic files including atomic coordinates, bond lengths and angles, and anisotropic thermal parameters for **3** (CIF). This material is available free of charge via the Internet at http://pubs.acs.org.

CM049431X